

# First hint for CP violation in neutrino oscillations from upcoming superbeam and reactor experiments

PATRICK HUBER<sup>a</sup>, MANFRED LINDNER<sup>b</sup>,  
THOMAS SCHWETZ<sup>c</sup>, AND WALTER WINTER<sup>d</sup>

<sup>a</sup> *Department of Physics, IPNAS, Virginia Tech, Blacksburg, VA 24061, USA*

<sup>b,c</sup> *Max-Planck-Institut für Kernphysik, Postfach 103980, D-69029 Heidelberg, Germany*

<sup>d</sup> *Institut für Theoretische Physik und Astrophysik, Universität Würzburg,  
D-97074 Würzburg, Germany*

## Abstract

We compare the physics potential of the upcoming neutrino oscillation experiments Daya Bay, Double Chooz, NO $\nu$ A, RENO, and T2K based on their anticipated nominal luminosities and schedules. After discussing the sensitivity to  $\theta_{13}$  and the leading atmospheric parameters, we demonstrate that leptonic CP violation will hardly be measurable without upgrades of the T2K and NO $\nu$ A proton drivers, even if  $\theta_{13}$  is large. In the presence of the proton drivers, the fast track to hints for CP violation requires communication between the T2K and NO $\nu$ A collaborations in terms of a mutual synchronization of their neutrino-antineutrino run plans. Even in that case, upgrades will only discover CP violation in a relatively small part of the parameter space at the  $3\sigma$  confidence level, while 90% confidence level hints will most likely be obtained. Therefore, we conclude that a new facility will be required if the goal is to obtain a significant result with high probability.

---

<sup>a</sup>Email: pahuber-at-vt.edu

<sup>b</sup>Email: lindner-at-mpi-hd.mpg.de

<sup>c</sup>Email: schwetz-at-mpi-hd.mpg.de

<sup>d</sup>Email: winter-at-physik.uni-wuerzburg.de

# 1 Introduction

Neutrino oscillations have been firmly established in the last ten years or so by a beautiful series of experiments with neutrinos from the sun [1–6], the Earth’s atmosphere [7, 8], nuclear reactors [9, 10], and accelerators [11, 12]. While these measurements have discovered and confirmed the dominant effective 2-flavor oscillation modes, it will be the purpose of the upcoming generation of experiments to discover sub-leading effects. This includes the following tasks:

1. Determination of the small lepton mixing angle  $\theta_{13}$ ,
2. Establishing CP violation (CPV) in neutrino oscillations for a value of the Dirac CP phase  $\delta_{\text{CP}} \neq 0, \pi$ ,
3. Identification of the type of the neutrino mass hierarchy (MH), which can be normal ( $\Delta m_{31}^2 > 0$ ) or inverted ( $\Delta m_{31}^2 < 0$ ).

There are several neutrino oscillation experiments currently under construction, which are expected to start data taking soon. These are the reactor neutrino experiments Double Chooz [13], Daya Bay [14], RENO [15] and the accelerator experiments T2K [16] and NO $\nu$ A [17]. The primary goal for all of these experiments is the discovery of the yet unknown mixing angle  $\theta_{13}$ . In this work, we will revisit the nominal sensitivities of these projects to  $\theta_{13}$  taking care of the different nature of the experiments ( $\bar{\nu}_e$  disappearance in reactors versus  $\nu_\mu \rightarrow \nu_e$  or  $\bar{\nu}_\mu \rightarrow \bar{\nu}_e$  appearance in accelerators), and estimate the time evolution of the global discovery reach for  $\theta_{13}$  based on the official schedules of the experiments. This analysis updates previous works [18–22] with respect to the now settled parameters for the considered experiments. Let us mention that eventually already the currently running experiments MINOS [12, 23] and OPERA [24] might give a first hint for a non-zero value of  $\theta_{13}$  in case it is close to the present bound. We do not consider these experiments here, but focus on the above facilities currently under preparation, since they will clarify such hints with high significance.

Furthermore, we will study if there is any chance to address items 2 and 3 above (CPV and MH) already with this set of upcoming experiments in case of a soon coming positive signal for  $\theta_{13}$ , which implies that  $\theta_{13}$  is relatively “large”. It turns out that even in this most favorable case the sensitivity to CPV and MH of these experiments in their nominal configuration is marginal. Therefore we will explore the potential of “minor upgrades” to the proposed setups of T2K and NO $\nu$ A, based upon mostly existing equipment. These include a longer running time and an upgraded beam power for both experiments, and the addition of antineutrino running in T2K. Furthermore, we investigate the optimization potential of a coordinated combination of T2K, NO $\nu$ A, and Daya Bay. The purpose of this analysis is to estimate whether there will be any chance to have information on CPV or the MH around 2022–2025, given the rather optimistic assumptions concerning beam performances and the size of  $\theta_{13}$ .

Such considerations are relevant in view of the current international effort towards a subsequent high precision neutrino facility [25, 26]. These studies aim for a decision point concerning a future facility around 2012, where improved information on  $\theta_{13}$  should be

Setup	$t_\nu$ [yF]	$t_{\bar{\nu}}$ [yF]	$P_{\text{Th}}$ or $P_{\text{Target}}$	$L$ [km]	Detector technology	$m_{\text{Det}}$
Double Chooz	-	3	8.6 GW	1.05	Liquid scintillator	8.3 t
Daya Bay	-	3	17.4 GW	1.7	Liquid scintillator	80 t
RENO	-	3	16.4 GW	1.4	Liquid scintillator	15.4 t
T2K	5	-	0.75 MW	295	Water Cerenkov	22.5 kt
NO $\nu$ A	3	3	0.7 MW	810	TASD	15 kt

**Table 1:** Summary of the standard setups at their nominal luminosities.

available from the above mentioned experiments. If a non-zero value is established until then, an eminent question will be whether CPV and MH can be found by upgrades of the existing experiments, or indeed a new facility will be necessary.

The outline of the paper is as follows. In Sec. 2, we describe the planned experiments and give some details on our simulations. In Sec. 3, we consider the nominal configurations of the experiments based on the information the experimental collaborations provide. We study the sensitivity to  $\theta_{13}$  (discovery potential as well as the case of large  $\theta_{13}$ ) and the improvements to be expected in the leading atmospheric parameters  $\theta_{23}$  and  $|\Delta m_{31}^2|$ . In Sec. 4, we discuss the prospective time evolution of the sensitivity to  $\theta_{13}$  within the upcoming years. In Sec. 5, we consider possible upgrades for T2K and NO $\nu$ A focusing on the measurements of CPV and MH in the case of relatively large  $\theta_{13}$ . Note that we arranged the Secs. 3 to 5 in an order from the most to the least established in terms of the data provided by the experimental collaborations. Summary and conclusions follow in Sec. 6. In the technical appendix we give details on our neutrino/antineutrino optimization algorithm.

## 2 Experiment descriptions and simulation methods

Below we describe in some detail the considered experimental setups and our simulation which we perform by using the GLOBES software [27, 28]. The corresponding `g1b`-files are available at the GLOBES web-page [27] including detailed technical information on the simulation. In all cases our strategy is to follow as close as possible the original Letters of Intent (LOIs) or Technical Design Reports (TDRs). We have made sure that our sensitivities agree with the “official” curves from the corresponding collaborations under the same assumptions. Table 1 summarizes the key parameters of the considered experiments.

Reactor experiments look for the disappearance of  $\bar{\nu}_e$ , governed by  $\theta_{13}$ , where the neutrinos are produced in the nuclear fission processes in commercial nuclear power plants. All three experiments, Double Chooz, Daya Bay, and RENO, use a liquid scintillator doped with Gadolinium in order to exploit the coincidence of a positron and a neutron from the reaction  $\bar{\nu}_e + p \rightarrow e^+ + n$ . The two crucial parameters determining the final sensitivity are the total exposure (proportional to the detector mass times the time-integrated thermal power of the reactor over the lifetime of the experiment) and the systematic uncertainty, see, *e.g.*, Ref. [20] for a discussion. All three proposals use the concept of near and far detectors in order to reduce uncertainties on the initial neutrino flux. Our implementation of systematic uncertainties is similar to the one of Ref. [29]. While for Double Chooz and Daya Bay detailed proposals are available, Refs. [13] and [14], respectively, the RENO experiment

is somewhat less documented and some properties have to be extrapolated from the other two proposals. The characteristics of the three reactor experiments are (see also Ref. [30] for a comparison study):

**Double Chooz:** The Chooz power plant in France consists of two reactors with 4.3 GW thermal power each. There will be two detectors with 8.3 t fiducial mass each, a far detector at a distance of 1.0 km and 1.1 km from the two cores, and a near detector at a distance of 470 m and 350 m, respectively. Including efficiencies of 80%, detector dead times, and a load factor of 78% for the reactors, the event rates per year are  $8 \times 10^4$  and  $1.5 \times 10^4$  for the near and far detectors, respectively. The uncertainty on the relative normalization of the detectors is assumed to be 0.6%.

**Daya Bay:** The Chinese Daya Bay reactor complex consists currently of two pairs of reactor cores (Daya Bay and Ling Ao), separated by about 1.1 km. The complex generates 11.6 GW of thermal power; this will increase to 17.4 GW by early 2011 when a third pair of reactor cores (Ling Ao II) is put into operation. For the 3 years nominal exposure we assume that all the mentioned six cores are operational. In total, eight detector modules will be installed, 20 t fiducial mass each. The far site consists of 4 modules with distances from the three reactors of 1.985, 1.613, and 1.618 km. There will also be two near labs, each containing two detector modules at distances from the reactors between 360 and 530 m. The event rate per year is about  $4 \times 10^5$  at the near sites and about  $10^5$  at the far site. The detector normalization is assumed to be 0.18% uncorrelated between the detector modules. This corresponds to the final goal in terms of systematics without swaping detector modules.

**RENO:** The RENO experiment will be located at the Yonggwang reactor complex in South Korea, which consists of 6 cores equally distributed along a straight line of about 1.5 km, with a total thermal power of 16.4 GW. Two detectors with about 15 t fiducial mass each will be installed roughly at distances of 320 m and 1.4 km from the reactor line. Event rates per year will be about  $6 \times 10^5$  at the near site and about  $3 \times 10^4$  at the far site. The relative detector normalization is assumed at 0.5%.

The T2K and NO $\nu$ A superbeam experiments search for the appearance of electron neutrinos in a beam of mainly muon neutrinos, from the decay of pions and kaons produced at a proton accelerator. Such beams unavoidably contain some intrinsic electron neutrinos which consist a background for the appearance search. Both experiments explore the off-axis technique to suppress the electron neutrino as well as the neutral current backgrounds and to achieve a more peaked beam spectrum. For both experiments, we also include the disappearance channels.

**T2K:** The T2K experiment [16] sends a neutrino beam from the J-PARC accelerator to the Super-Kamiokande water Cerenkov detector with a fiducial mass of 22.5 kt at a distance of 295 km. Our simulation is based on publicly accessible sources as of 2008. We assume a 2.5 degree off-axis beam corresponding to 0.75 MW of beam power for 5 years of neutrino running. The analysis of the  $\nu_e$  appearance follows the thesis of M. Fechner [31]. Event rates and spectra for total signal and total background

match Fig. 6.8 of Ref. [31], and systematics are taken from chapter 6 of that reference. Our sensitivity from the appearance channel agrees with Fig. 6.17 of Ref. [31]. The disappearance analysis is taken from a talk by I. Kato given at Neutrino 2008 [32]. From that source we obtain rates and spectra for signal and non-QE background.

**NO $\nu$ A:** The description of NO $\nu$ A concerning the  $\nu_e/\bar{\nu}_e$  appearance signals follows the proposal as of March 15, 2005 [17], the description of the disappearance signal is taken from Ref. [33]. We calibrated our event simulation to the numbers for signal, background, and efficiencies given in the October 2007 TDR [34] (Tabs. 6.2–6.4). NO $\nu$ A is a Totally Active Scintillator Detector (TASD) with a mass of 15 kt and is located at a distance of 810 km from NUMI beam source at Fermilab. The nominal luminosity is  $18 \times 10^{20}$  protons on target for neutrinos and antineutrinos, each. This number of protons on target is assumed to correspond to 3 years running at 0.7 MW beam power. While this equal exposure to neutrinos and antineutrinos is the default assumption, we will also consider the sensitivities in case of neutrino running only in some of the next sections. We adopt systematical errors of 5% on the signal (not stated in the TDR) and 10% on the background (as given in the TDR). We use an analysis energy window from 1 to 3 GeV and assume the so-called medium energy (ME) beam configuration.

For the sensitivity analyses we use the oscillation parameter values from Ref. [35]:  $\Delta m_{21}^2 = 7.65 \cdot 10^{-5} \text{ eV}^2$ ,  $|\Delta m_{31}^2| = 2.40 \cdot 10^{-5} \text{ eV}^2$ ,  $\sin^2 \theta_{12} = 0.304$ , and  $\sin^2 \theta_{23} = 0.500$ , unless stated otherwise. We impose external  $1\sigma$  errors on  $\Delta m_{21}^2$  (3%) and  $\theta_{12}$  (4%) as conservative estimates for the current measurement errors [35], as well as  $\Delta m_{31}^2$  (5%) for reactor experiments if analyzed without beam experiments. In addition, we include a 2% matter density uncertainty.

### 3 Physics potential at nominal luminosities

In this section, we discuss the physics potential of the experiments listed in Table 1 based on their nominal luminosities, *i.e.*, the running times, detectors masses, and total numbers of protons (or thermal reactor powers) anticipated by the respective collaborations.

#### 3.1 Discovery potentials for $\theta_{13}$ , MH, and CPV

We show the discovery potentials for  $\theta_{13}$ , MH, and CPV in Fig. 1. These discovery potentials quantify for any given (true)  $\sin^2 2\theta_{13}$  for which fraction of possible (true) values of  $\delta_{\text{CP}}$  the corresponding quantity will be discovered.<sup>1</sup> For  $\theta_{13}$  this means excluding the value  $\theta_{13} = 0$ . The mass hierarchy discovery potential is defined as the ability to exclude any degenerate solution for the wrong (fit) hierarchy at the chosen confidence level. Similarly, the CP violation discovery potential refers to the ability to exclude the CP conserving solutions  $\delta_{\text{CP}} = 0$  and  $\delta_{\text{CP}} = \pi$  for any degenerate solution at the chosen confidence level. These discovery potentials of course depend on the true values of  $\theta_{13}$  and  $\delta_{\text{CP}}$  and the true

---

<sup>1</sup>In this work we use the terms *true value* and *simulated value* synonymously in order to denote the values of parameters adopted to generate “data”, in contrast to the *fit values* used to fit these data.

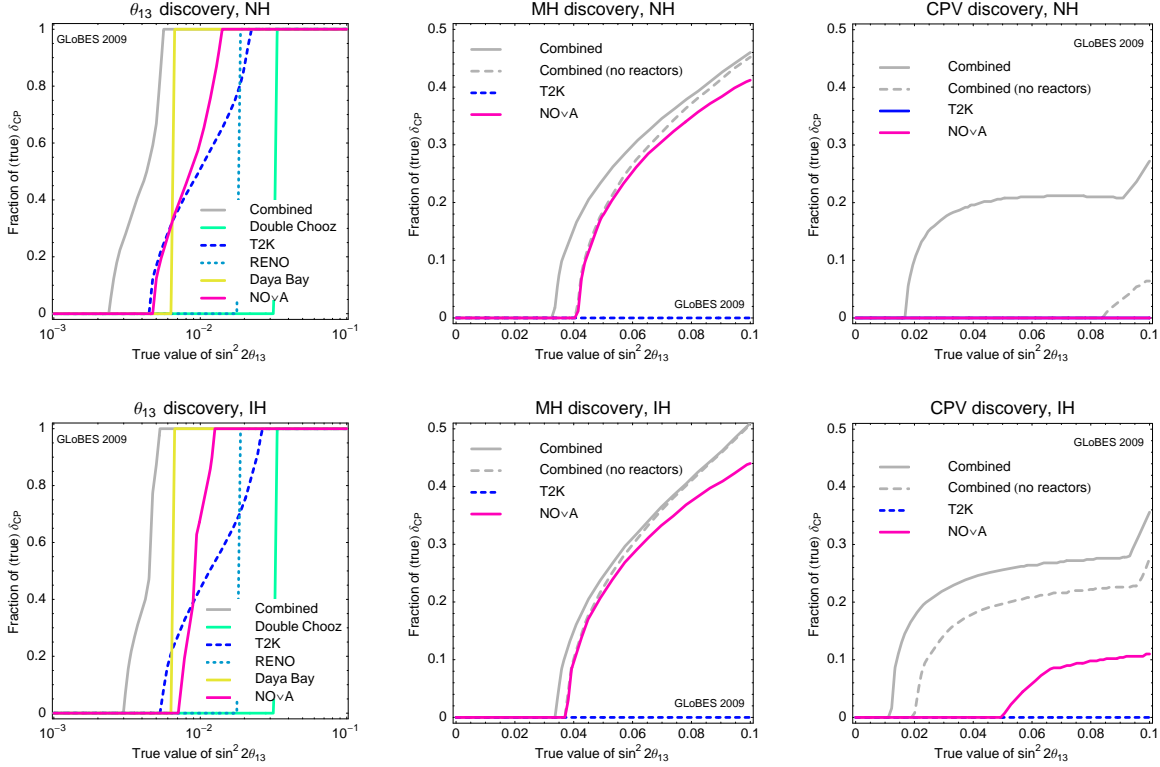


**Figure 1:**  $\theta_{13}$ , MH, and CPV discovery potential as fraction of true  $\delta_{CP}$  as a function of the true  $\sin^2 2\theta_{13}$  for the normal hierarchy (upper row) and inverted hierarchy (lower row) at the 90% CL. Note the different vertical scales in the different panels.

hierarchy. In Fig. 1 we show for a given true value of  $\sin^2 2\theta_{13}$  (horizontal axis) and a given true hierarchy (upper row normal, lower row inverted) the fraction of all possible true values of  $\delta_{CP}$  for which the discovery can be achieved at the 90% confidence level. Hence, a fraction of  $\delta_{CP}$  of unity (or 100%) for a given  $\sin^2 2\theta_{13}$  corresponds to a discovery for any possible value of  $\delta_{CP}$ .

The  $\theta_{13}$  discovery potential (*cf.*, left panels of Fig. 1) of the reactor experiments does not depend on  $\delta_{CP}$  since by convention this phase does not appear in the disappearance probability  $P_{ee}$ . Furthermore, the probability is given to good approximation by an effective 2-flavor expression:  $P_{ee}^{\text{react}} \approx 1 - \sin^2 2\theta_{13} \sin^2(\Delta m_{31}^2 L/4E)$ . Thanks to the large exposure, Daya Bay will have the best discovery potential among the reactor experiments of  $\sin^2 2\theta_{13} = 0.0066$  at the 90% CL, compared to 0.018 for RENO and 0.033 for Double Chooz.<sup>2</sup> In contrast, the  $\nu_{\mu} \rightarrow \nu_e$  appearance probability relevant for the beam experiments shows a

<sup>2</sup>Let us mention that the Daya Bay assumptions of a systematical error of 0.18%, fully uncorrelated among all detectors is more aggressive than for other reactor experiments. For example, if the systematic error is at the level of 0.6%, such as assumed in Double Chooz, the Daya Bay sensitivity of  $\sin^2 2\theta_{13} = 0.0066$  deteriorates to  $\sin^2 2\theta_{13} \simeq 0.01$ . If on the other hand the systematic error is 0.38% and assumed to be fully correlated among modules at one site the limit would  $\sin^2 2\theta_{13} \simeq 0.012$  [36]. See also the discussion in Ref. [30].

dependence on the CP phase due to an interference term of the oscillations with  $\Delta m_{31}^2$  and  $\Delta m_{21}^2$ . A discussion of the complementarity of reactor and beam experiments can be found, *e.g.*, in Refs. [18,20,22]. Whether the best  $\theta_{13}$  discovery potential is obtained from Daya Bay or from one of the beams depends on the true  $\delta_{\text{CP}}$ . For instance, for the normal hierarchy, T2K and NO $\nu$ A will have a discovery potential for slightly smaller values of  $\sin^2 2\theta_{13}$  than Daya Bay for about 30% of all possible  $\delta_{\text{CP}}$  values.

The mass hierarchy measurement (*cf.*, middle panels of Fig. 1) requires NO $\nu$ A because of its relatively long baseline and therefore significant matter effects. T2K does not have any mass hierarchy discovery potential. For very large  $\sin^2 2\theta_{13}$ , the mass hierarchy will be discovered for about 40–50% of all values of  $\delta_{\text{CP}}$  at 90% CL. There is no sensitivity left at this CL for  $\sin^2 2\theta_{13} < 0.04$ . Only minor improvement can be achieved if other experiments are added to NO $\nu$ A; the combination with T2K helps somewhat for large  $\theta_{13}$ , whereas the reactor experiments contribute somewhat for small  $\theta_{13}$ .

For the discovery of CP violation (*cf.*, right panels of Fig. 1), neither T2K nor NO $\nu$ A alone have a substantial potential. Only the combination of these two experiments can measure CPV at 90% CL for up to 30% of all values of  $\delta_{\text{CP}}$  if the hierarchy is inverted. This hierarchy dependence appears because the matter effect in NO $\nu$ A leads to a more balanced neutrino-antineutrino statistics for the inverted hierarchy due to an matter enhancement of the antineutrino event rate. In the presence of the reactor experiments, however, the CP violation discovery potential improves significantly, especially for the normal hierarchy. If the hierarchy is normal, Daya Bay may in fact be the key prerequisite to obtain an early hint for CP violation.

We stress that these sensitivities for MH and CPV are at the 90% CL, which by no means can be considered as a discovery. Increasing the CL leads to drastic loss in sensitivity and almost nothing can be said about CPV and MH at the  $3\sigma$  CL.

### 3.2 The case of $\theta_{13}$ just around the corner

We show in Fig. 2 (normal simulated hierarchy) and Fig. 3 (inverted simulated hierarchy) how typical fits in the  $\theta_{13}$ - $\delta_{\text{CP}}$  plane would look like if  $\theta_{13}$  was large ( $\sin^2 2\theta_{13} = 0.1$ ) and  $\delta_{\text{CP}}$  was close to maximal CP violation  $\delta_{\text{CP}} = \pi/2$  (upper rows) and  $\delta_{\text{CP}} = 3\pi/2$  (lower rows). The fit contours for the right fit hierarchy are shaded (colored), the ones for the wrong fit hierarchy fit are shown as curves.<sup>3</sup>

The figures show the characteristics of the different classes of experiments: The reactor experiments do not depend on  $\delta_{\text{CP}}$ , and the wrong fit hierarchy coincides with the right hierarchy. For T2K, which is simulated with neutrino running only, there is some dependence on  $\delta_{\text{CP}}$ , but the correlation between  $\delta_{\text{CP}}$  and  $\theta_{13}$  cannot be resolved without antineutrino running. The wrong hierarchy contours are slightly shifted, but the minimum  $\chi^2$  is close to zero. NO $\nu$ A, on the other hand, has both neutrino and antineutrino running in our simulation, which means that the correlation can, at least in principle, be resolved. The wrong hierarchy can in some cases be excluded because of matter effects. In the combination of the experiments, the combination between Daya Bay and the beams allows for a substantial

---

<sup>3</sup>Here the “right” fit hierarchy is the same as the simulated hierarchy, and the “wrong” fit hierarchy is the other fit hierarchy.

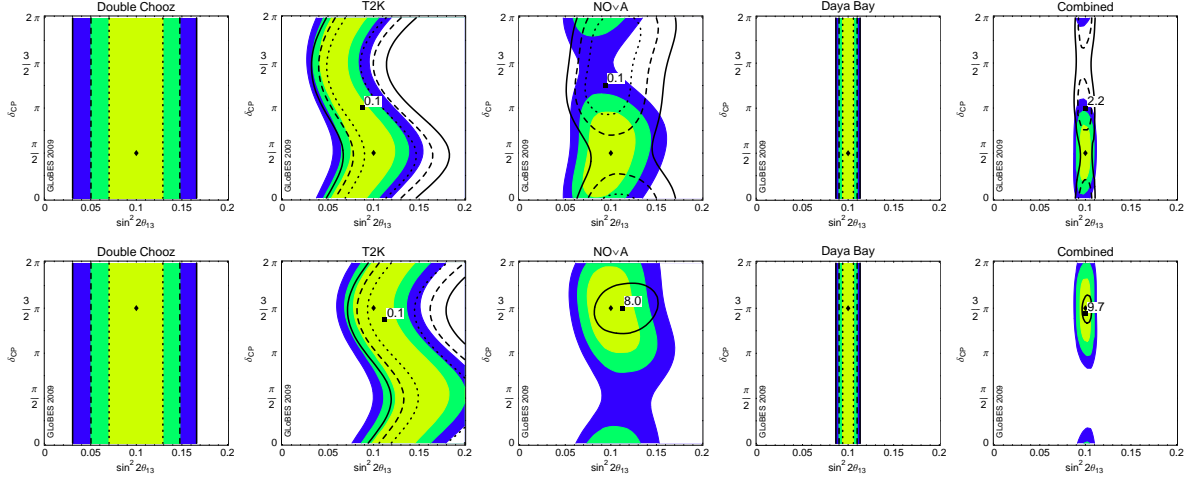


**Figure 2:** Fits in the  $\theta_{13}$ - $\delta_{CP}$  plane for  $\sin^2 2\theta_{13} = 0.1$  and  $\delta_{CP} = \pi/2$  (upper row) and  $\delta_{CP} = 3\pi/2$  (lower row). A normal simulated hierarchy is assumed. The contours refer to  $1\sigma$ ,  $2\sigma$ , and  $3\sigma$  (2 d.o.f.). The fit contours for the right fit hierarchy are shaded (colored), the ones for the wrong fit hierarchy fit are shown as curves. The best-fit values are marked by diamonds and boxes for the right and wrong hierarchy, respectively, where the minimum  $\chi^2$  for the wrong hierarchy is explicitly shown.

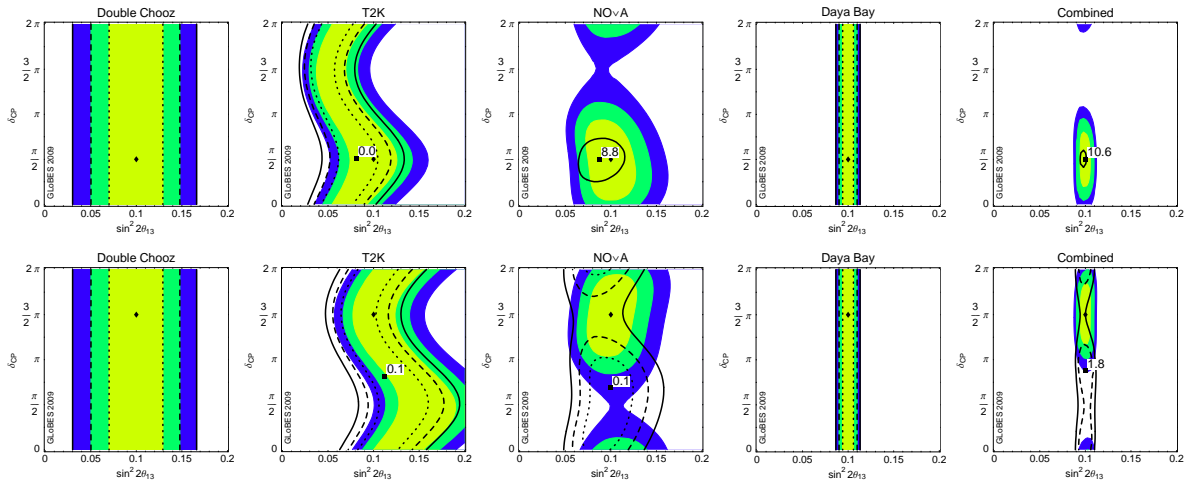


**Figure 3:** Same as Fig. 2, for the inverted simulated hierarchy.



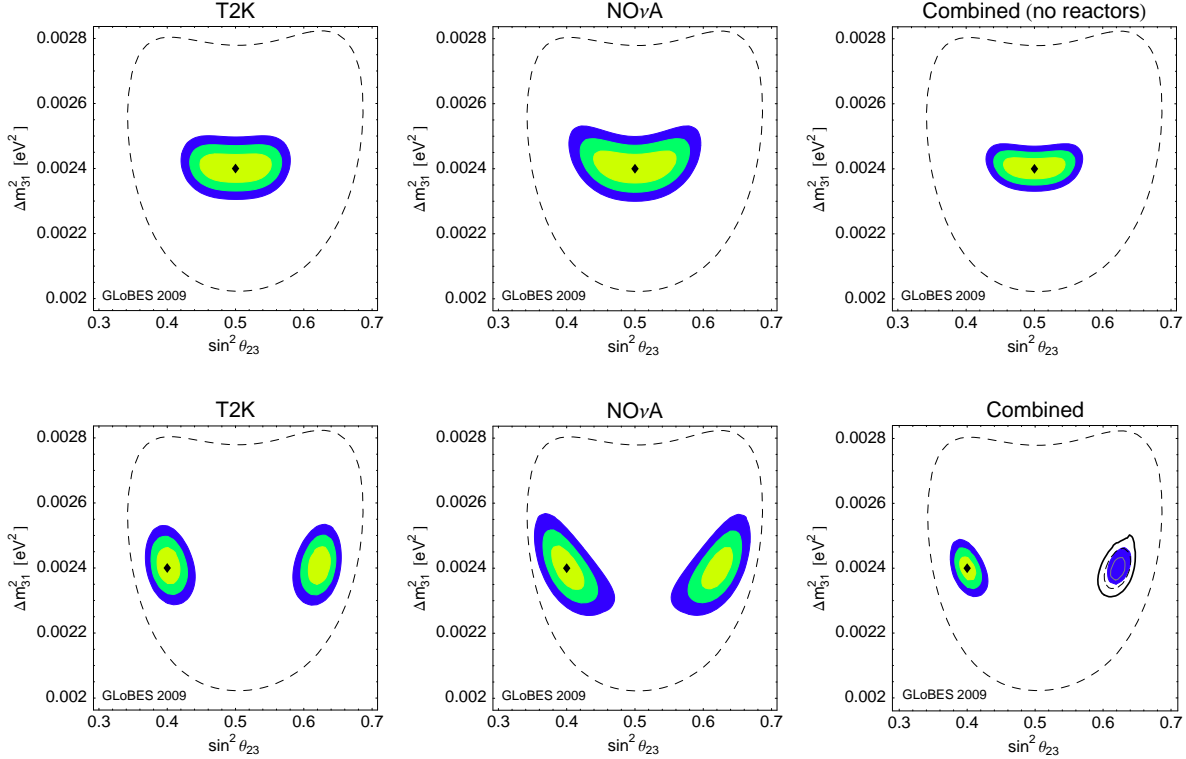


**Figure 4:** Fits in  $\sin^2 \theta_{23}$ - $\Delta m_{31}^2$  plane for two different sets of simulated values:  $\sin^2 \theta_{23} = 0.5$ ,  $\sin^2 2\theta_{13} = 0$  (upper row) and  $\sin^2 \theta_{23} = 0.4$ ,  $\sin^2 2\theta_{13} = 0.1$ ,  $\delta_{\text{CP}} = 0$  (lower row). The upper right panel does not change significantly if the reactor experiments are added. In the lower right panel, the unshaded contours are for the combination of all experiments without reactor experiments. The currently allowed MINOS+atmospheric region is shown as dashed curves in all panels ( $3\sigma$  confidence level) [35]. The contours corresponds to the  $1\sigma$ ,  $2\sigma$ , and  $3\sigma$  confidence level, respectively (2 d.o.f.).

reduction of the allowed parameter space due to almost orthogonal measurements. In the most optimistic cases, the mass hierarchy can be determined at  $3\sigma$  confidence level, and maximal CP violation can be established at relatively modest confidence as well. However, note that these optimistic cases represent only a very small fraction of the parameter space.

### 3.3 Leading atmospheric parameters

No matter if  $\theta_{13}$  will be discovered or not, the upcoming beam experiments will allow for precision measurements of the leading atmospheric parameters by exploring the  $\nu_\mu$  disappearance channel. We illustrate the improvement of the currently allowed parameter range (dashed curves) in the  $\sin^2 \theta_{23}$ - $\Delta m_{31}^2$  plane in Fig. 4 for the two different scenarios  $\sin^2 \theta_{23} = 0.5$ ,  $\sin^2 2\theta_{13} = 0$  (upper row) and  $\sin^2 \theta_{23} = 0.4$ ,  $\sin^2 2\theta_{13} = 0.1$ ,  $\delta_{\text{CP}} = 0$  (lower row). In the maximal mixing case, the allowed region can be substantially reduced by the beam experiments, especially the  $\Delta m_{31}^2$  interval, with hardly any dependence on the reactor experiments or the value of  $\theta_{13}$ .

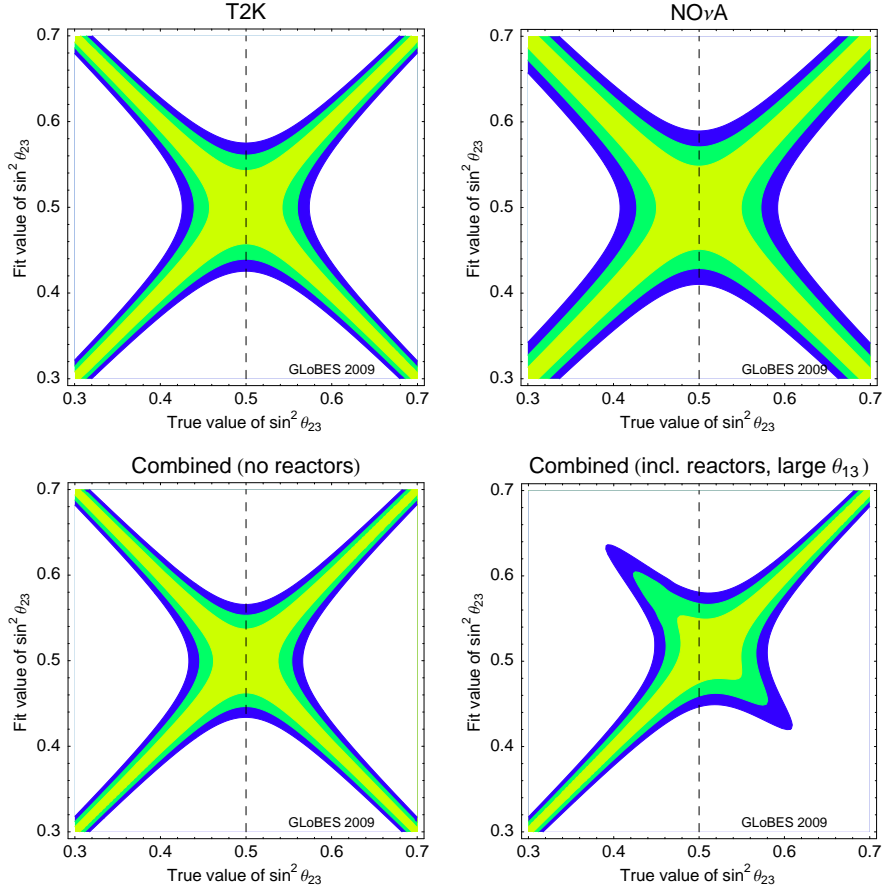


**Figure 5:** Fit range in  $\theta_{23}$  as a function of the true  $\theta_{23}$  for different experiments ( $1\sigma$ ,  $2\sigma$ ,  $3\sigma$  for 1 d.o.f.). The upper left and right, and the lower left panels are computed for  $\sin^2 2\theta_{13} = 0$ , whereas the lower right panel is for  $\sin^2 2\theta_{13} = 0.1$ ,  $\delta_{\text{CP}} = 0$ . The qualitative picture is hardly affected by the reactor experiments or large  $\theta_{13}$ , unless both conditions apply (large  $\theta_{13}$  and reactor experiments).

In the lower row of Fig. 4, a relatively large deviation from maximal atmospheric mixing is chosen. Again, the allowed parameter ranges can be significantly reduced by the beams, apart from an octant ambiguity in  $\theta_{23}$  [37]. As illustrated in the lower right panel this ambiguity might be resolved if  $\theta_{13}$  is large and beams are combined with an accurate reactor experiment, compare the shaded (including reactors) and unshaded (excluding reactors) regions. In this case the two solutions corresponding to the two  $\theta_{23}$ -octants for the appearance channel of the beams are located at rather different values of  $\theta_{13}$ . Therefore, an independent determination of  $\theta_{13}$  from reactors can in principle resolve the ambiguity [18, 22].

In order to discuss the sensitivity of deviations from maximal atmospheric mixing and the octant resolution potential as a function of the true  $\theta_{23}$ , we show in Fig. 5 the fit range in  $\theta_{23}$  as a function of the true  $\theta_{23}$  for different experiments. Deviations from maximal atmospheric mixing are theoretically interesting because they may point towards deviations from a symmetry, see Ref. [38] for a more detailed discussion. In Fig. 5, such a deviation can be established if  $\sin^2 \theta_{23} = 0.5$  can be excluded at the vertical axis. Obviously, this

measurement does not require the presence of the reactor experiments or large  $\theta_{13}$ . The combination of the beams can establish deviations from maximal atmospheric mixing for  $|\sin^2 \theta_{23} - 0.5| \gtrsim 0.07$  ( $3\sigma$ ).

The sensitivity to the octant of  $\theta_{23}$  can be interesting to distinguish certain models. For instance, sum rules such as  $\theta_{23} \simeq \pi/4 \pm \theta_{13}^2/2$  might be tested, where the sign depends on the model assumptions [39]. If deviations from maximality are due to renormalization group effects, in a large class of models the sign of the deviation is different for normal and inverted hierarchy, and depends on the presence of Supersymmetry [40]. As illustrated by the lower two panels in Fig. 5, both the combination with the reactor data and a large  $\theta_{13}$  are necessary to perform this measurement with the given experiments. Sensitivity to the octant of  $\theta_{23}$  is present if any  $\theta_{23}$  in the wrong octant can be excluded. There is no octant sensitivity in the upper and lower left panels of Fig. 5. From the lower right panel, we can read off octant sensitivity if  $\sin^2 \theta_{23} \lesssim 0.39$  or  $\sin^2 \theta_{23} \gtrsim 0.61$  ( $3\sigma$ ,  $\sin^2 2\theta_{13} = 0.1$ ).

## 4 Sensitivity time evolution

In the following, we discuss the sensitivity evolution within the coming years for different experiments, based as much as possible on official statements of the collaborations. Although the assumed schedules and proton beam plans may turn out to be not realistic in some cases, our toy scenario will be illustrative to show the key issues for the individual experiments within the global neutrino oscillation context. We will show the sensitivities as a function of time assuming that data are continuously analyzed and results are available immediately. The key assumptions for our toy scenario are as follows.

**Double Chooz** starts 09/2009 and runs 1.5 years with far detector only, then with far and near detector [41]. We assume that the experiment ends after five years.

**Daya Bay** Starts 07/2011. At this time, it is assumed that near and far detector halls are completed, and all modules are ready [42]. Furthermore, all three pairs of reactor cores are assumed to be online. Again, we limit the operation time to five years.

**RENO** starts 06/2010 [43] with both detectors and runs for 5 years.

**T2K** starts 09/2009 with virtually 0 MW beam power, which increases linear to 0.75 MW reached in 12/2012. From then we assume the full target power of 0.75 MW. (This is an approximation for the T2K proton plan from Ref. [44]). The Super-Kamiokande detector is online from the very beginning and the beam runs with neutrinos only, (at least) until 2018 or 2019.

**NO $\nu$ A** starts 08/2012 with full beam (0.7 MW), but 2.5 kt detector mass only. Then the detector mass increases linearly to 15 kt in 01/2014. From then we assume the full detector mass of 15 kt [45]. The beam runs with neutrinos first, until the equivalent of three years operation at nominal luminosity (*cf.*, Table 1) is reached, *i.e.*, 03/2016. Then it switches (possibly) to antineutrinos and runs at least until 2019.

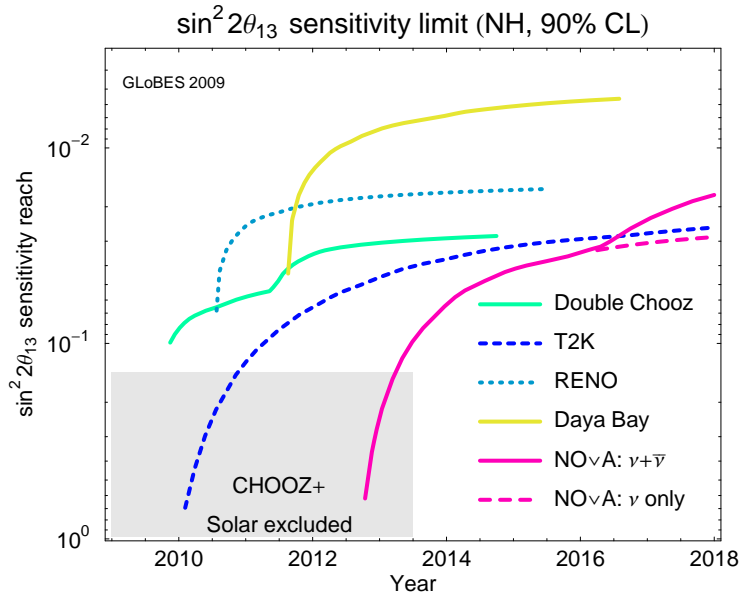


**Figure 6:** Evolution of the  $\theta_{13}$  sensitivity limit as a function of time (90% CL), *i.e.*, the 90% CL limit which will be obtained if the true  $\theta_{13}$  is zero.

#### 4.1 Finding versus constraining $\theta_{13}$

We now discuss the sensitivity of the different experiments to  $\theta_{13}$ . We include two qualitatively different aspects in the discussion: The  $\theta_{13}$  sensitivity limit and the  $\theta_{13}$  discovery potential. The  $\theta_{13}$  sensitivity limit describes the ability of an experiment to constrain  $\theta_{13}$  if no signal is seen. It is basically determined by the worst case parameter combination which may fake the simulated  $\theta_{13} = 0$ . The sensitivity limit does not depend on the simulated hierarchy and  $\delta_{CP}$ , as the simulated  $\theta_{13} = 0$ . For a more detailed discussion, see Ref. [21], App. C. The  $\theta_{13}$  discovery potential is given by the smallest true value of  $\theta_{13} > 0$  which cannot be fitted with  $\theta_{13} = 0$  at a given CL. Since the simulated  $\theta_{13}$ ,  $\delta_{CP}$ , and hierarchy determine the simulated rates, the  $\theta_{13}$  discovery potential will depend on the values of all these parameters chosen by nature. On the other hand, correlations and degeneracies are of minor importance because for the fit  $\theta_{13} = 0$  is used. The smallest  $\theta_{13}$  discovery potential for all values of  $\delta_{CP}$  and the MH (risk-minimized  $\theta_{13}$  discovery potential) is often similar to the  $\theta_{13}$  sensitivity limit. This holds to very good approximation for reactor experiments, where statistics are Gaussian and the oscillation physics is simple. For beam experiments differences occur due to Poisson statistics as well as more complicated oscillation physics implying correlations and degeneracies.

We show the  $\theta_{13}$  sensitivity limit as a function of time in Fig. 6. We observe that the global sensitivity limit will be dominated by reactor experiments. As soon as operational, Daya Bay will dominate the global limit. For Daya Bay, time is not critical, but matching the systematics or statistics goals is. If the assumed schedules of both, Double Chooz and Daya Bay are matched, Double Chooz will dominate the  $\theta_{13}$  sensitivity for about two years in the absence of RENO. If available, RENO, on the other hand, will dominate the  $\theta_{13}$

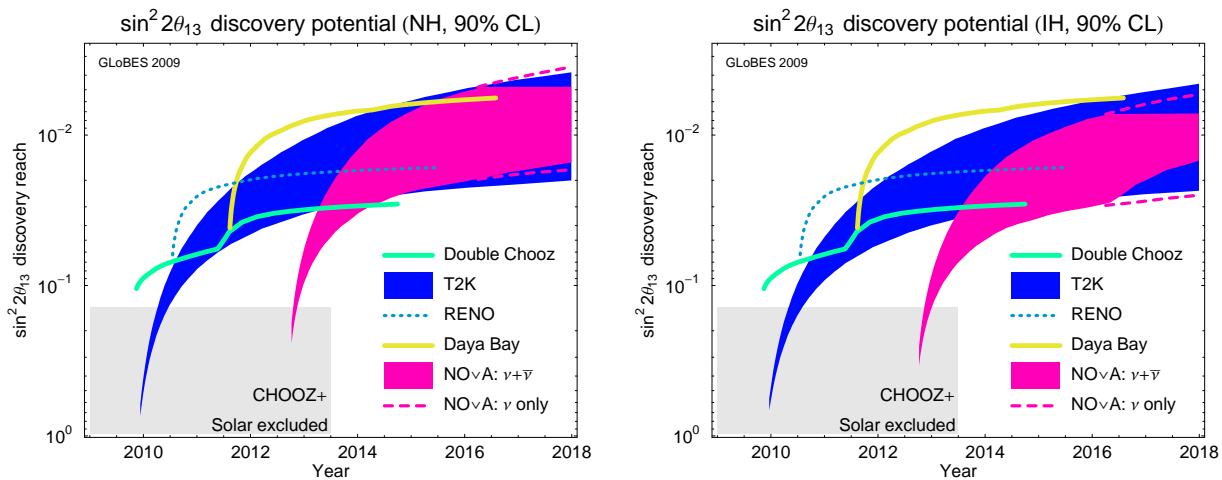


**Figure 7:** Evolution of the  $\theta_{13}$  discovery potential as a function of time (90% CL), *i.e.*, the smallest value of  $\theta_{13}$  which can be distinguished from zero at 90% CL. We assume the normal and inverted simulated hierarchies in the left and right panels, respectively. The bands reflect the (unknown) true value of  $\delta_{CP}$ .

sensitivity if it is operational significantly before the end of 2011. Since we do not obtain any CP violation or mass hierarchy sensitivity before 2014, as we shall demonstrate later, the reactor contribution to those will be completely dominated by Daya Bay. As a peculiarity, the  $\theta_{13}$  sensitivity of NO $\nu$ A is improved by switching to antineutrinos. However, the global limit will at that time be dominated by the reactor experiments.

The  $\theta_{13}$  discovery potential is shown in Fig. 7 as a function of time. For the beam experiments, the dependence on the true value of  $\delta_{CP}$  is shown as shaded region, whereas the reactor experiments are not affected by the true  $\delta_{CP}$ . There is a small dependence on the true mass hierarchy for the beam experiments, compare left and right panels. The comparison of Figs. 7 and 6 shows that suitable values of  $\delta_{CP}$  may significantly improve the discovery potential of beams compared to their sensitivity limit. Indeed, the beam experiments may discover  $\theta_{13}$  for smaller  $\theta_{13}$  than Daya Bay in a small fraction of the parameter space (see also Fig. 1). Overall, it may however be more likely that the reactor experiments are faster. The NO $\nu$ A bands become more narrow for some additional antineutrino running, which means that the best case potential gets slightly worse, but the worst case becomes somewhat better. Again, this may not be an argument for antineutrino running since the anticipated Daya Bay sensitivity may not be exceed-able. For a more detailed discussion of the potential antineutrino running, we refer to Sec. 5.

Note that this discussion is based on the unitarity standard three-flavor oscillation framework. If the search for new physics is taken into account, different reactor experiments, or reactor experiments and superbeams, may imply different information and therefore be very complementary; see, *e.g.*, Refs. [46, 47].

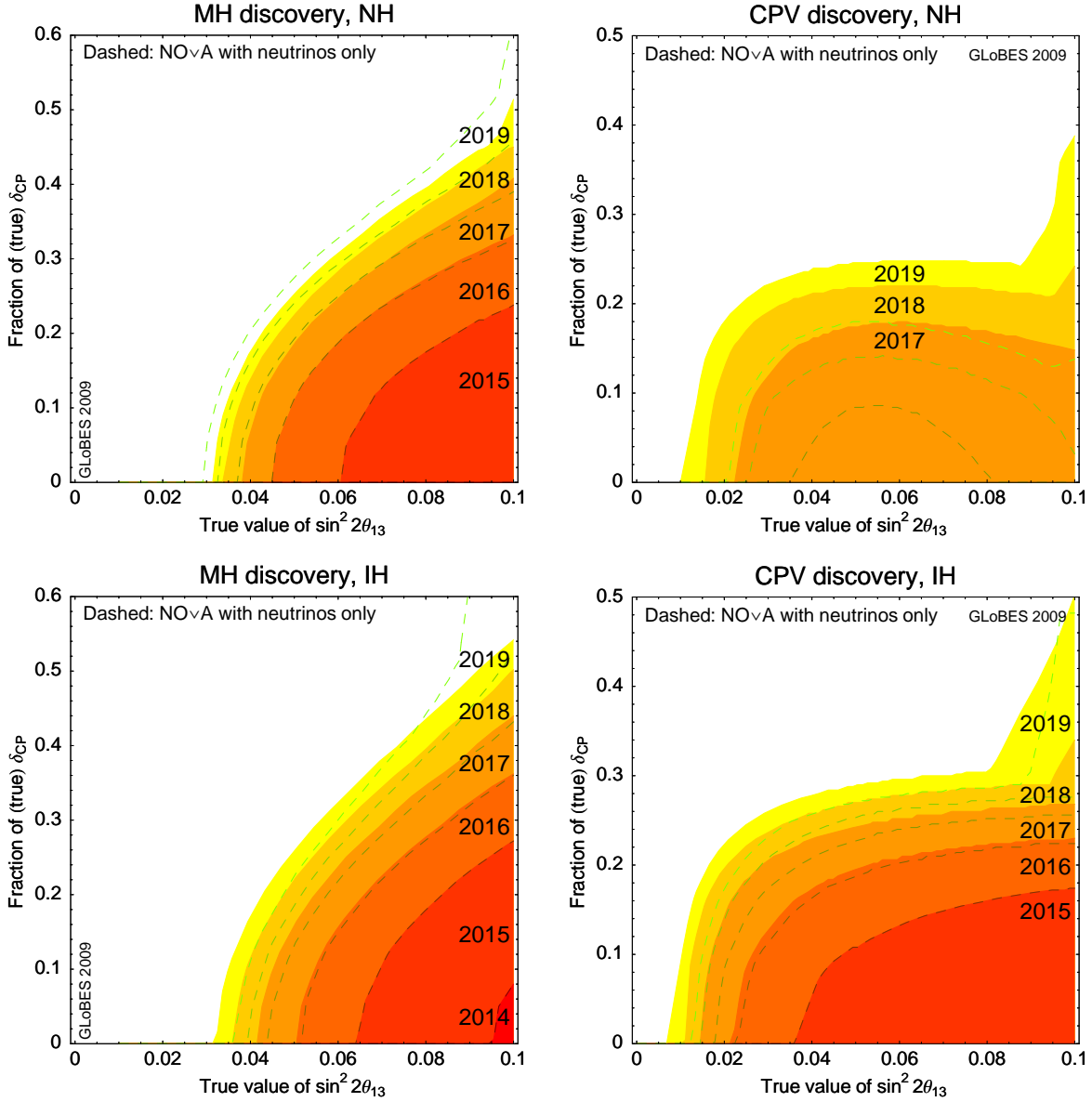


**Figure 8:** Mass hierarchy (left panels) and CP violation (right panels) discovery potentials as a function of true  $\sin^2 2\theta_{13}$  and fraction of true  $\delta_{CP}$  at 90% CL from T2K, NO $\nu$ A and reactor data. The upper row corresponds to the normal simulated hierarchy, the lower row to the inverted simulated hierarchy. The different shadings correspond to different points of time, as marked in the plots (note that “2015” here means mid 2015). The dashed curves refer to NO $\nu$ A with neutrino running only, whereas the shaded contours refer to the nominal NO $\nu$ A neutrino-antineutrino plan. If no contour is shown for a specific year, there is no sensitivity. Note the different scales on the vertical axes.

## 4.2 Mass hierarchy and CP violation discovery potentials

We show in Fig. 8 the mass hierarchy (left panels) and CP violation (right panels) discovery potentials as a function of true  $\sin^2 2\theta_{13}$  and fraction of (true)  $\delta_{\text{CP}}$  from T2K, NO $\nu$ A, and Daya Bay. The upper row corresponds to the normal simulated hierarchy, the lower row to the inverted simulated hierarchy. The different contours represent different points in time, and can be viewed as timeslices. Obviously, there will be no mass hierarchy discovery before 2014, and no CP violation discovery before 2015. In the most optimistic case without upgrades, the mass hierarchy and CP violation can be discovered in about 50% of all cases of  $\delta_{\text{CP}}$  by 2019. Note, however, that we show the 90% CL potentials here, whereas there is only extremely poor  $3\sigma$  sensitivity. Therefore, as a first conclusion, there will be no high significance determination of the mass hierarchy or CP violation without the next generation of experiments. In the most optimistic case, some hints may be obtained in about 2015-2018. As discussed earlier (*cf.*, Fig. 1), NO $\nu$ A plays a key role in these discovery potentials.

As far as the NO $\nu$ A switching to antineutrinos is concerned, we show in Fig. 8 the case if NO $\nu$ A runs with neutrinos only as dashed curves. As expectable, for CP violation the antineutrino run is mandatory. For the mass hierarchy discovery, however, it is of secondary importance. For a more detailed discussion, see Sec. 5.

Interesting observations can be obtained from the comparison between Fig. 8 and the  $\theta_{13}$  time evolution. If  $\sin^2 2\theta_{13} \lesssim 0.02$ , it may already be excluded by Daya Bay early 2012 (*cf.*, Fig. 6). In this case, it will be clear already before the NO $\nu$ A startup that there is no chance to find the mass hierarchy or CP violation without significant upgrades or new experiments. On the other hand, if  $\sin^2 2\theta_{13} \gtrsim 0.02$ , this will be known at about the same time (*cf.*, Fig. 7), meaning that NO $\nu$ A has a realistic chance to see something. In this way, the “branching point” 2012 will be an interesting point of time at which strategic decisions on the future neutrino oscillation program can be made, such as in favor of upgrades or a new high intensity facility.

## 5 Beam upgrades for large $\theta_{13}$ and the $\nu$ - $\bar{\nu}$ optimization

In the previous sections we have seen that the sensitivity to CPV and MH of the discussed experiments in their nominal configuration as defined in Sec. 2 is marginal, at best. In this section we address the following question. Imagine that a finite value of  $\theta_{13}$  is discovered soon; can “modest upgrades” of the experiments considerably improve the sensitivity to CPV and MH? With “modest upgrades” we mean modifications of existing equipment and infrastructure. This includes a longer running time and an upgraded beam power for both accelerator experiments and the addition of antineutrino running in T2K.<sup>4</sup> It does not include new beam lines or new detectors. In particular, our toy scenario is the following:<sup>5</sup>

**T2K** We assume that a proton driver is installed, which increases the beam power from 0.75 to 1.66 MW, linearly from 2015 to 2016 [49].

<sup>4</sup>The anti-neutrino running beam fluxes for the 2.5 degree off-axis beam for T2K are taken from [48].

<sup>5</sup>In this section, if not stated otherwise, years denote always the middle of year, *i.e.*, 2019 = July 1st, 2019.

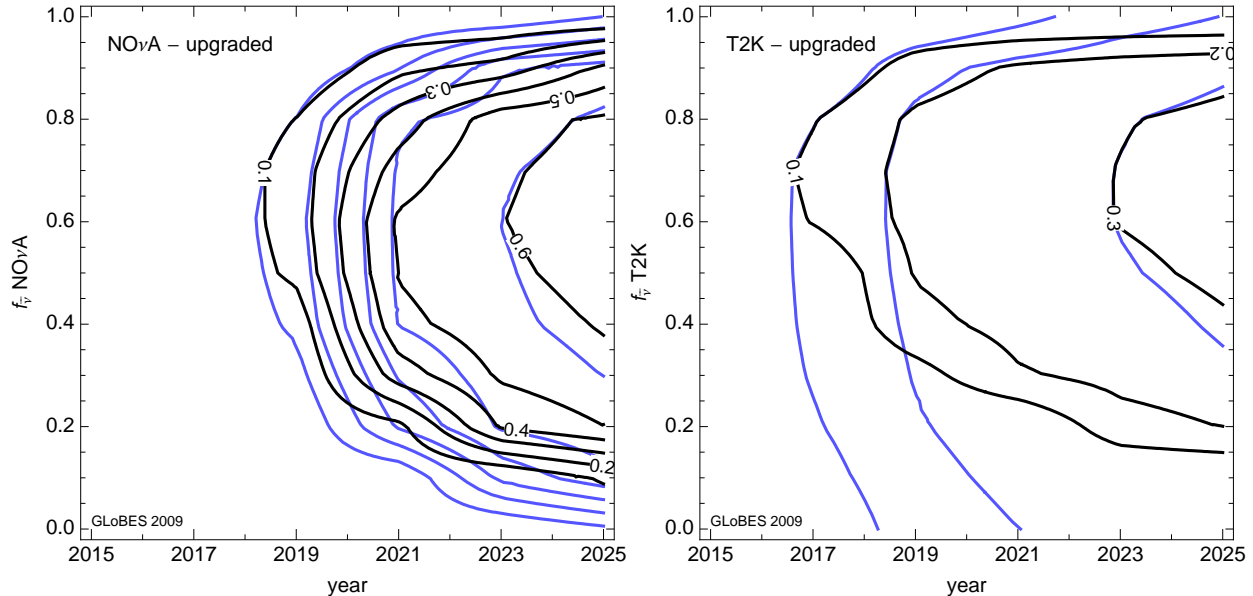


**Figure 9:** The contours show the CP fraction for which CP violation can be established at 90% CL as a function of the year and the fraction of antineutrino running  $f_{\bar{\nu}}$  up to that year. We assume the upgraded run plan. The black contours assume T2K (right hand panel) or NO $\nu$ A (left hand panel) data only, whereas the colored contours show the result for the case where reactor data on  $\theta_{13}$  is included.

**NO $\nu$ A** At Fermilab, the proton driver “ProjectX” is discussed. We assume a linear increase from 0.7 to 2.3 MW from March 2018 to March 2019 [50].

For Double Chooz, in principle, there exists the upgrade option to Triple Chooz [29]. However, from Fig. 6, we do not see how that could compete with Daya Bay (either timescale-wise, or physics-wise). Therefore, we do not discuss this possibility here. Likewise, neither for RENO nor for Daya Bay upgrade options are discussed/anticipated.

To be specific, we assume in the following that the true value of  $\theta_{13}$  is  $\sin^2 2\theta_{13} = 0.1$  and the true hierarchy is normal. According to Fig. 7 this value of  $\theta_{13}$  will be discovered before 2011 by Double Chooz, T2K and RENO. We focus first on CPV and comment on the MH in Sec. 5.3.

### 5.1 Optimization of neutrino/antineutrino running

We start our analysis by discussing the optimization of the fraction of neutrino/antineutrino exposures. Fig. 9 shows the fraction of  $\delta_{CP}$ -values for which CPV can be established at 90% CL as a function of time and as a function of the fraction of antineutrino running  $f_{\bar{\nu}}$  for NO $\nu$ A (left) and T2K (right). Here,  $f_{\bar{\nu}} = 0(1)$  corresponds to the full exposure with neutrinos (antineutrinos). As expected, in order to address CPV a sizable fraction of antineutrino running is required:  $f_{\bar{\nu}} = 0.6 - 0.7$  for T2K and  $f_{\bar{\nu}} = 0.5 - 0.6$  for NO $\nu$ A. The plot is for normal hierarchy, but results are similar for inverted hierarchy. Without reactor data  $f_{\bar{\nu}} = 0$  is strongly disfavored even when the beams are upgraded, indicating



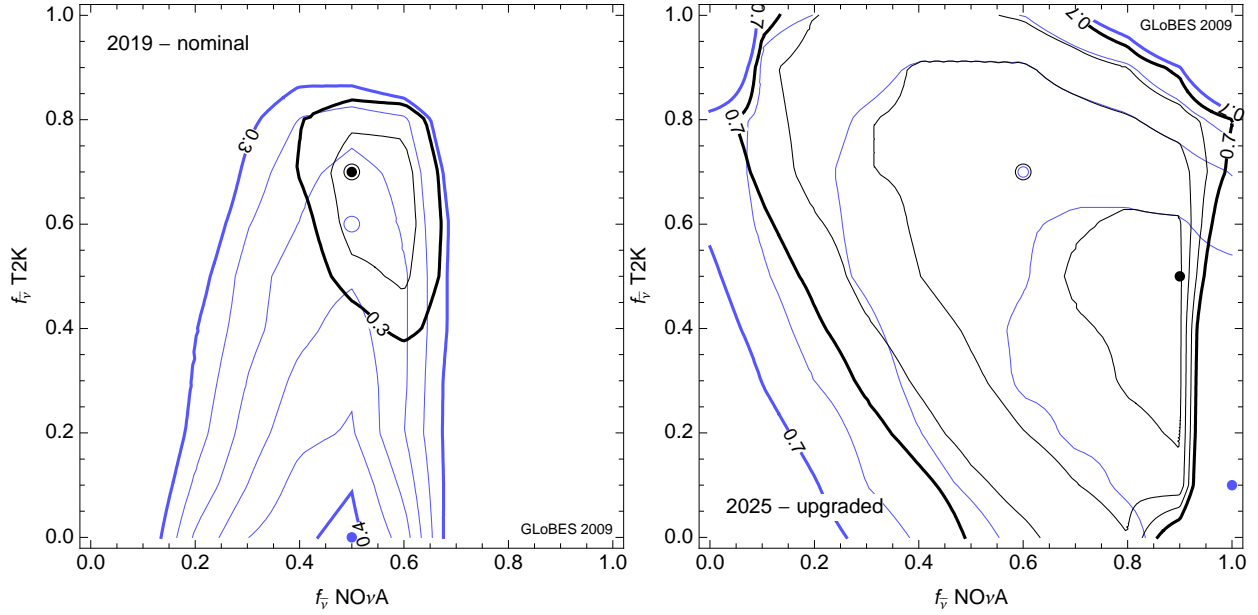


**Figure 10:** The contours show the CP fraction for which CP violation can be established at 90% CL as a function of the antineutrino fraction in NO $\nu$ A and T2K in the year 2019 assuming the nominal run plan (left hand panel) or in the year 2025 with the upgraded run plan (right hand panel). The black contours assume the combined data from NO $\nu$ A and T2K only, whereas for the colored contours also reactor data on  $\theta_{13}$  is included. The thick contours have a spacing of 0.1 whereas the thin contours have a spacing of 0.02. The black disk denotes the optimal point for beam data only and whereas the colored disk denotes the optimal point for beam and reactor data combined. The circles denote the optima found for each experiment individually.

that spectral information is not enough to provide a measurement of  $\delta_{\text{CP}}$ .

NO $\nu$ A with upgrades reaches a CP fraction of about 60%, while T2K achieves only about 30%. The reason is that the beam upgrade is a factor of 3.2 for NO $\nu$ A whereas it is only 2.2 for T2K. Moreover, antineutrino running is very difficult for T2K due to the low beam energy. Since the ratio of antineutrino/neutrino cross sections as well as fluxes decreases with energy, statistics is rather poor for T2K antineutrino data. This is especially true for the 2.5 $^\circ$  off-axis T2K beam. Optimization of beam optics or energy is beyond the scope of this work.

The blue (light gray) curves in Fig. 9 show the case when reactor data on  $\theta_{13}$  are combined with that of the beam experiment. While for NO $\nu$ A, reactor data have only a minor impact, for T2K, the combination with a reactor experiment can considerably relax the requirement on  $f_{\bar{\nu}}$  and even replace the antineutrino running altogether in most cases [51]. However, the optimal CPV fraction for T2K is not improved significantly by adding reactor data.

Fig. 10 shows the neutrino/antineutrino optimization for the combined data of T2K and NO $\nu$ A, with and without reactor data. In the left panel we assume only the nominal luminosities for the beams, but allow for an arbitrary fraction of antineutrinos for both experiments. Without reactor data, the optimum is at  $f_{\bar{\nu}}^{\text{NO}\nu\text{A}}/f_{\bar{\nu}}^{\text{T2K}} = 0.5/0.7$ . The CP

fraction is about 32% and antineutrino data is required for both experiments. If reactor data are added, the optimum is at  $f_{\bar{\nu}}^{\text{NO}\nu\text{A}}/f_{\bar{\nu}}^{\text{T2K}} = 0.5/0$ , which is remarkably close to the nominal plan for the experiments. The CP fraction is 40%, in agreement with Fig. 8. We observe again that reactor data are more useful than the statistically weak antineutrino data in T2K, which means that it is preferable to fully explore neutrino data in T2K.

The right panel of Fig. 10 shows the same analysis for the upgraded beams. The tendency is to use large antineutrino fractions in NO $\nu$ A and less in T2K, the optimum being  $f_{\bar{\nu}}^{\text{NO}\nu\text{A}}/f_{\bar{\nu}}^{\text{T2K}} = 0.9/0.5$  (1/0.1) without (with) reactors. We find an optimal CP sensitivity at 90% CL for beam+reactor data for about 76% of all  $\delta_{\text{CP}}$  values. The landscape becomes rather flat and similar CP fractions can be obtained for a wide range of antineutrino fractions.

## 5.2 Optimal run plan

In the previous subsection we investigated the optimal total fraction of antineutrino running for the full lifetime of the experiment. In this section, we proceed further and ask the following question: what is the neutrino/antineutrino running strategy such that at *at each point in time* the optimal sensitivity to CPV is obtained? Let us first define a reference neutrino-antineutrino scenario (“nominal run plan”) as follows:

**Phase I: Until design luminosity reached** T2K: neutrinos only, NO $\nu$ A: 50% neutrinos followed by 50% antineutrinos (such as in LOIs)

**Phase II: After design luminosity reached until mid 2025** T2K: 50% neutrinos followed by 50% antineutrinos. NO $\nu$ A: 50% neutrinos followed by 50% antineutrinos

Note that the definition of phase I and II is not connected with the upgrade point of time, but the design luminosity. The  $\delta_{\text{CP}}$  fractions for CPV at 90% CL for this nominal run plan are shown in Fig. 11 as a function of time with blue bands, where light and dark colors indicate neutrino and antineutrino running, respectively.

Now we investigate whether a globally optimized neutrino-antineutrino run plan has the potential to improve the performance with respect to this reference plan. This (non-deterministic) optimization is performed with the help of a genetic algorithm described in detail in appendix A. Roughly, the algorithm evolves a set of switching times between neutrinos and antineutrinos for T2K and NO $\nu$ A by favoring “individuals” with the largest CP fraction at each point in time and disfavoring the ones with too many switching points. After evolving a randomly chosen population of 2000 individuals for 50 generations we average over the 100 “fittest” individuals. The results of this optimization search are shown as green bands in Fig. 11, see also Tab. 3 in the appendix.

Let us first discuss the nominal exposures without the beam upgrades (upper row of panels). We find that the reference  $\nu$ - $\bar{\nu}$  run plan outlined above provides a very suboptimal performance and can delay physics by four to five years for beam data without reactors. If reactor data are added, delays will be reduced to one or two years. Again we observe that reactor data allow to avoid antineutrino running in T2K, and we find that an early antineutrino run in NO $\nu$ A is preferred. The optimal strategy is not costly in terms of switches, only one or two additional switches are required.

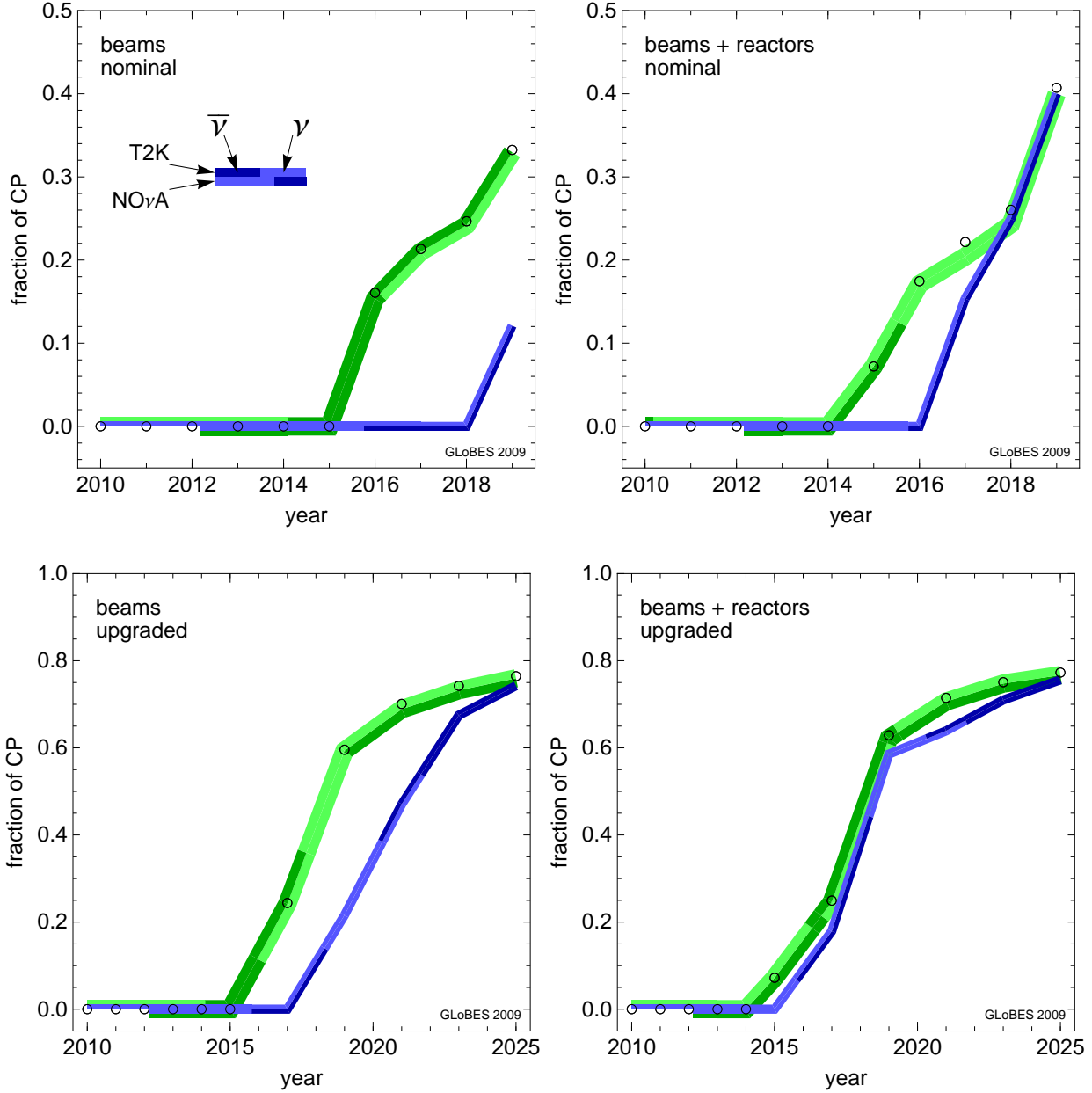


**Figure 11:** Fraction of  $\delta_{CP}$  values for which CP violation can be discovered at 90% CL as a function of time for the nominal run plan (upper row) and the upgraded run plan (lower row). These plots assume the true sign of  $\Delta m_{31}^2 > 0$ . The left hand column shows the results for a combination of T2K and NOνA alone, whereas the right hand column includes reactor data. The green band is for the globally optimal run plan, whereas the blue band is for the nominal run plan. Light and dark colors indicate neutrino and antineutrino running, respectively. The black circles denote the absolute maximal performance for a given time.

The lower panels in Fig. 11 show the results for upgraded beams. Again the reference  $\nu\text{-}\bar{\nu}$  run plan provides a suboptimal performance and can delay physics by two to three years for beam data only. Inclusion of reactor data helps a lot and delays are reduced to one year. Here reactor data no longer allow for circumventing antineutrino running in T2K. We observe that the final overall performance with and without reactors is very similar if the run plan is optimized. Thus, it seems that one should strive to optimize the beams as much as possible on their own. In that way the reactor data can be used as an independent cross check of the result, for instance, to provide some sensitivity to non-standard neutrino physics. Again we find that the optimal strategy prefers early antineutrino data from NO $\nu$ A, and that only one or two additional switches are required.

### 5.3 Time evolution of physics potential

Having optimized the CPV performance for a true value  $\sin^2 2\theta_{13} = 0.1$  in the previous subsections, we now relax this assumption<sup>6</sup> and discuss the sensitivities of these optimized configurations as a function of  $\theta_{13}$ . We consider the upgraded beams for T2K and NO $\nu$ A combined with reactor data, and show results for CPV as well as for the neutrino mass hierarchy. Fig. 12 shows the discovery potential as a function of true  $\sin^2 2\theta_{13}$  and fraction of true  $\delta_{\text{CP}}$  for times from 2015 to 2025. The upper row of this figure shows the discovery potentials at the 90% CL. These results can be compared to Fig. 8 (upper panels), where one should note the different scales on the vertical axes. Obviously, with the optimal upgrade plan, there is a significant improvement of the MH and CPV discovery potentials. At the 90% confidence level, there will be hints for the MH and CPV for  $\sin^2 2\theta_{13} \gtrsim 0.05$  for most values of  $\delta_{\text{CP}}$  around 2025.

However, certainly a 90% CL is not sufficient to make any meaningful statement about a discovery. Therefore, we show in the lower row of Fig. 12 the corresponding results at  $3\sigma$  CL. Obviously the sensitivity regions reduce drastically, however, we see from the figure that assuming both beams upgraded, a fully optimized neutrino/antineutrino run plan, and data from reactors a non-negligible discovery potential at  $3\sigma$  will be reached in 2025. The mass hierarchy can be identified for  $\sin^2 2\theta_{13} \gtrsim 0.05$  for about 20% to 40% of  $\delta_{\text{CP}}$  values, whereas CPV can be discovered for  $\sin^2 2\theta_{13} \gtrsim 0.02$  for 25% of  $\delta_{\text{CP}}$  values. In both cases, MH and CPV, there is sensitivity for values of  $\delta_{\text{CP}}$  around  $3\pi/2$  ( $\pi/2$ ) if the true hierarchy is normal (inverted). This behaviour is visible in Figs. 2 and 3 and it is related to the sign of the matter effect, see, *e.g.*, Ref. [52] for a discussion.

Let us mention that in the previous two subsections we have optimized the sensitivity to CPV. However, it turns out that this is also very close to the optimal performance for the MH determination. Furthermore, it is a feature of our optimization plan that the performance in the case of a (true) inverted hierarchy is similar to one for the normal hierarchy. Therefore it is not shown explicitly here.

---

<sup>6</sup>Note, that in general the  $\chi^2$ -functions will have lower values and hence be less steep for smaller  $\theta_{13}$ . Therefore, optimization is less crucial and a wider range of running fractions is acceptable. Thus a solution which was optimal for large  $\theta_{13}$  will still be very close to optimal for somewhat smaller  $\theta_{13}$ . However, all sensitivities will be decreased.

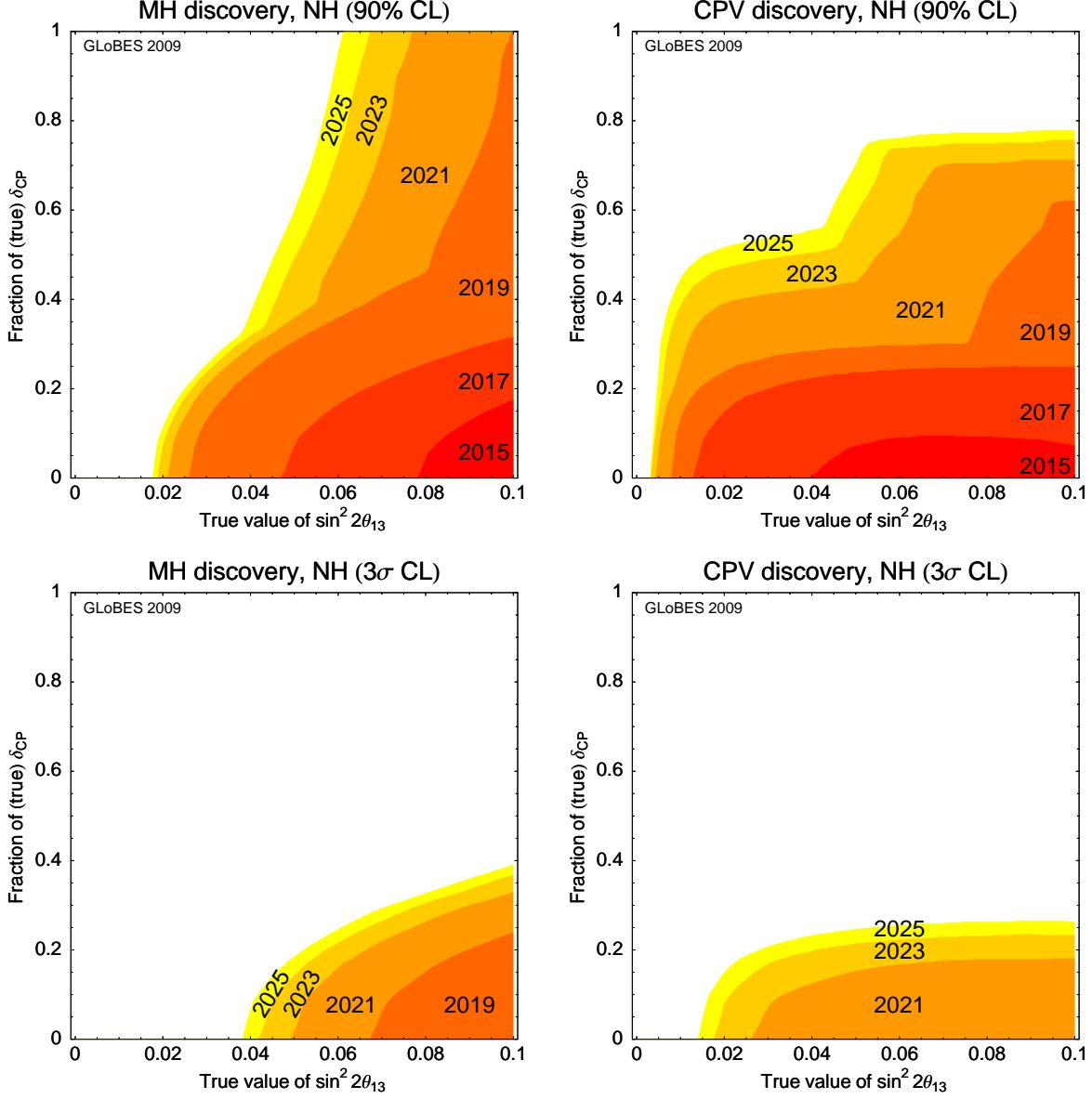


**Figure 12:** Mass hierarchy (left panels) and CP violation (right panels) discovery potentials as a function of true  $\sin^2 2\theta_{13}$  and fraction of (true)  $\delta_{CP}$  for our optimal run plan including upgrades and reactor experiments; *cf.*, Table 3. The upper panels are for 90% CL, the lower panels for  $3\sigma$  CL. The different shadings corresponds to different points of time, as marked in the plots. Note the different scales on the vertical axes compared to Fig. 8.

	$\sin^2 2\theta_{13}$	$ \Delta m_{31}^2 $	$ \sin^2 \theta_{23} - 0.5 $
Double Chooz	0.033 (0.060)	–	–
T2K	0.004–0.027 (0.011–0.040)	+2.0% (+3.7%) –1.9% (–3.5%)	0.055 (0.074)
RENO	0.018 (0.033)	–	–
Daya Bay	0.007 (0.012)	–	–
NO $\nu$ A	0.005–0.014 (0.011–0.025)	+2.5% (+4.7%) –2.0% (–3.6%)	0.065 (0.092)

**Table 2:** Summary of nominal sensitivities at 90% ( $3\sigma$ ). We show the discovery potential for  $\sin^2 2\theta_{13}$  (where for the beams we give the best and worst sensitivity depending on  $\delta_{\text{CP}}$  and mass hierarchy), the accuracy on  $|\Delta m_{31}^2|$  (for maximal mixing), and the sensitivity to deviations from maximal  $\theta_{23}$  mixing.

## 6 Summary and conclusions

In this work we have discussed the physics potential of the upcoming neutrino oscillation experiments Double Chooz, Daya Bay, RENO, T2K, and NO $\nu$ A. In the first part we have reconsidered the sensitivities from their nominal exposures, such as stated in the experimental proposals. These results are summarized in Table 2. While Double Chooz and maybe RENO could allow for a fast discovery of a relatively large value of  $\theta_{13}$ , the ultimate reactor experiment will be Daya Bay, which will dominate a few months after it comes online. The  $\theta_{13}$  performance of the beam experiments will depend on the value of  $\delta_{\text{CP}}$  and the performance indicator. In the case of no signal, the limit on  $\theta_{13}$  will be similar to the one from Double Chooz, whereas a favorable value of  $\delta_{\text{CP}}$  will allow for a discovery for slightly smaller  $\theta_{13}$  than Daya Bay.

We have found that the global sensitivity to CP violation and the neutrino mass hierarchy of all experiments with nominal exposures is marginal. For the largest allowed values of  $\theta_{13}$ , typically a hint at 90% CL can be obtained for about 25% to 50% of all possible values of  $\delta_{\text{CP}}$ , while almost nothing can be said at  $3\sigma$ . Therefore, we have investigated the possibilities to increase the sensitivity by minor upgrades of the beam experiments in case  $\theta_{13}$  is not too far from its present bound and hence discovered soon. These upgrades are based on existing equipment and include an increase of beam power with the help of proton drivers, longer running times, and the addition of antineutrino running in T2K. We have performed an optimization study concerning the distribution of neutrino and antineutrino data runs in T2K and NO $\nu$ A in order to maximize the global sensitivity reach. We have found that typically communication between the two beam experiments will improve the overall sensitivity. For example, the optimal sensitivity usually requires relatively early antineutrino data from NO $\nu$ A. Furthermore, we have found that the sensitivity of the optimized running strategy for T2K plus NO $\nu$ A is rather similar to the one with reactor experiment data used in addition.

These results are summarized in Fig. 12. Assuming both beams upgraded, a fully optimized neutrino/antineutrino run plan, and data from reactors, we have found that a hint for CP violation at 90% CL can be obtained around 2025 for a large fraction of  $\delta_{\text{CP}}$  for a reasonably large  $\theta_{13}$ . However, the discovery potential for CP violation and mass hierarchy drastically reduces at the  $3\sigma$  CL. Nevertheless, a non-negligible discovery potential at  $3\sigma$  will be reached in 2025: The mass hierarchy can be identified for  $\sin^2 2\theta_{13} \gtrsim 0.05$  for about

20% to 40% of  $\delta_{\text{CP}}$  values, whereas CP violation can be discovered for  $\sin^2 2\theta_{13} \gtrsim 0.02$  for 25% of  $\delta_{\text{CP}}$  values. Sensitivity to the mass hierarchy and CP violation is obtained for values of  $\delta_{\text{CP}}$  close to maximal CP violation:  $\delta_{\text{CP}} \simeq 3\pi/2$  ( $\pi/2$ ) for a true normal (inverted) hierarchy, but not for the opposite case.

Let us mention that NO $\nu$ A dominates the MH determination and typically also has a somewhat better sensitivity than T2K for CPV. For example, at  $\sin^2 2\theta_{13} = 0.1$ , NO $\nu$ A alone obtains a CP fraction for CPV at 90% CL of about 60%, whereas T2K reaches 35%, and the combination yields 76% (both beams with upgrades). The reasons are that the beam upgrade we consider is a factor of 3.2 for NO $\nu$ A whereas it is only 2.2 for T2K, and antineutrino running is very difficult for T2K due to the low beam energy. Since the ratios of antineutrino/neutrino cross sections as well as fluxes decrease with energy, statistics is rather poor for T2K antineutrino data.

Our results raise the question on how to adapt the global oscillation strategy in case  $\theta_{13}$  were discovered soon. Although “minor upgrades” of existing facilities may provide a non-negligible sensitivity to CP violation and the mass hierarchy, there is high risk associated with this strategy, since for about 75% of all possible values for  $\delta_{\text{CP}}$  no discovery will be possible at the  $3\sigma$  level. In contrast, a high precision facility such as a wide band superbearm or a beta beam with very large detectors or a neutrino factory [25, 26] would certainly be able to perform a solid determination of CP violation and the mass hierarchy in case of such a large value of  $\theta_{13}$ . Therefore, we conclude that the upcoming generation of oscillation experiments may lead to interesting indications for the mass hierarchy and CP violation, but it is very likely that an experiment beyond the upcoming superbearms (including reasonable upgrades) will be required to confirm these hints.

## Acknowledgments

This work was supported by the European Union under the European Commission Framework Programme 07 Design Study EUROnu, Project 212372, and by the Transregio Sonderforschungsbereich TR27 “Neutrinos and Beyond” der Deutschen Forschungsgemeinschaft. WW also would like to acknowledge support from the Emmy Noether program of Deutsche Forschungsgemeinschaft, contract WI 2639/2-1.

## A Optimization method

Luminosity  $\mathcal{L}$  is given by the time integrated product of target mass  $m$  and beam power  $p$

$$\mathcal{L}(t) := \int_{t_0}^t dt' m(t') p(t'), \quad (1)$$

where we allow for  $m$  and  $p$  to be time dependent. We define the normalized luminosity  $L$  by

$$L(t) = \frac{\mathcal{L}(t)}{\mathcal{L}_0}, \quad (2)$$

where  $\mathcal{L}_0$  corresponds to the design luminosity of the experiment. Since, in the following we will discuss T2K and NO $\nu$ A every quantity pertaining to T2K will carry  $T$  as subscript

and those carrying subscript  $N$  pertain to  $\text{NO}\nu\text{A}$ .

T2K and  $\text{NO}\nu\text{A}$  both can run neutrinos or antineutrinos. We will denote the the fraction of antineutrinos in each experiment by  $f$ , where

$$f(t) = \frac{L_{\bar{\nu}}(t)}{L(t)}. \quad (3)$$

The current run plans foresee no antineutrino running for T2K,  $f_T^0 = 0$  and 50% of antineutrino running for  $\text{NO}\nu\text{A}$ ,  $f_N^0 = 0.5$ . For a given, true value of  $\sin^2 2\theta_{13}$  we can compute the obtainable fraction of  $\delta_{\text{CP}}$ ,  $\mathcal{C}$ , for the measurement of CP violation as a functions of both  $f_T$  and  $f_N$ . This is shown in figure 10. Of course this will be a time dependent quantity denoted by  $\mathcal{C}(f_N(t), f_T(t))$ . To simplify our notation we will write  $\mathcal{C}_t(f_N, f_T)$ . For algorithmic purposes, it turns out to be useful to define the normalized CP fraction  $C$  by

$$C_t(f_N, f_T) = \frac{\mathcal{C}_t(f_N, f_T)}{\hat{\mathcal{C}}_t} \quad \text{with} \quad \hat{\mathcal{C}}_t = \max_{f_N, f_T} \mathcal{C}_t(f_N, f_T). \quad (4)$$

Thus,  $C_t$  will have values from 0 to 1 for all times  $t$ . Note, that there will be separate and distinct  $\mathcal{C}_t$  and  $C_t$  for the true hierarchy normal (NH) or inverted (IH).

Since an experiment needs to reverse the polarity of the electric current in the focusing horn, its operation will be divided into phases of neutrino running and those of antineutrino running. Any such division can be described a set of times at which the operation mode switches, plus the initial running configuration. We will denote such a set as  $g = \{g_1, \dots, g_{l_g}\}$  for initial neutrino running and with  $\bar{g} = \{g_1, \dots, g_{l_{\bar{g}}}\}$  for initial antineutrino running. The  $g_i$  denote the individual switching times and  $l_g$  the total number of switches.  $g$  uniquely determines the the antineutrino fraction as a function of time

$$f_g(t) = \frac{L(t) - L(g_{k+1})}{L(t)} + \sum_{i=0}^{2i < k} \frac{L(g_{2i+1}) - L(g_{2i})}{L(t)} \quad \text{with} \quad g_{k+1} \leq t, \quad (5)$$

for starting with antineutrinos otherwise the sum starts at  $i = 1$ . Thus, we now can fix the value of  $C_t$  for any  $t$  by inserting the  $f_g(t)$  like this

$$\kappa(t, g_N, g_T) = C_t(f_{g_N}(t), f_{g_T}(t)), \quad (6)$$

in case both experiments started with neutrino running. Again, there are two functions  $\kappa^{NH}(t, g_N, g_T)$  for true hierarchy normal and  $\kappa^{IH}(t, g_N, g_T)$  for true hierarchy inverted. The goal now is to find a sequence of switching times  $g$  which yields  $\kappa^{NH}(t, g_N, g_T) = 1, \forall t$  and  $\kappa^{IH}(t, g_N, g_T) = 1, \forall t$ . In this case, we would have optimal sensitivity at any given moment in time, irrespective of the true mass hierarchy. We will search such  $g$  or  $\bar{g}$  by using a genetic algorithm. To this end, we define a fitness function to evaluate the relative performance of different sequences  $g$ .

$$\pi(g_N, g_T) = \frac{1}{\underbrace{\max\{1 - \kappa^{NH}(\tau_i, g_N, g_T), 1 - \kappa^{IH}(\tau_i, g_N, g_T)\}}_{=: \mu^{-1}}} \frac{1}{\underbrace{l_{g_N} + l_{g_T}}_{l^{-1}}}, \quad (7)$$



where the  $\tau_i$  are suitably chosen points in time, *e.g.* every two years from  $t_0$  on. The first term selects those solutions which manage to balance the deviation from optimal performance at all times. The second term penalizes solution which switch very frequently without gaining significantly in the first term. The genotype of each individual is given by a pair of  $\{g_N, g_T\}$ . In our implementation of the algorithm the length of each sequence  $l_{g_N}$  and  $l_{g_T}$  are free parameters and subject to evolution. We start with a population of widely varying sequence length. Thus, we do not have to specify the number of switches. Also, two times  $g_i$  and  $g_{i+1}$  are merged if they are less than a month apart. Each population consists of 2000 individuals which are evolved over 50 generations. We consider 4 populations

$$\{g_N, g_T\}, \{\bar{g}_N, g_T\}, \{g_N, \bar{g}_T\}, \{\bar{g}_N, \bar{g}_T\}. \quad (8)$$

The results for each population are shown in table 3. The  $\tau_i$  are

$$\{2010.5, 2011.5, 2012.5, 2013.5, 2014.5, 2015.5, 2016.5, 2017.5, 2018.5, 2019.5\}$$

for nominal luminosity and

$$\{2010.5, 2011.5, 2012.5, 2013.5, 2014.5, 2015.5, 2017.5, 2019.5, 2021.5, 2023.5, 2025.5\}$$

for upgraded luminosity.

## References

- [1] B. T. Cleveland *et al.*, *Astrophys. J.* **496**, 505 (1998).
- [2] M. Altmann *et al.* (GNO), *Phys. Lett.* **B616**, 174 (2005), [hep-ex/0504037](#).
- [3] J. Hosaka *et al.* (Super-Kamiokande), *Phys. Rev.* **D73**, 112001 (2006), [hep-ex/0508053](#).
- [4] Q. R. Ahmad *et al.* (SNO), *Phys. Rev. Lett.* **89**, 011301 (2002), [nucl-ex/0204008](#).
- [5] B. Aharmim *et al.* (SNO), *Phys. Rev. Lett.* **101**, 111301 (2008), [0806.0989](#).
- [6] C. Arpesella *et al.* (Borexino), *Phys. Rev. Lett.* **101**, 091302 (2008), [0805.3843](#).
- [7] Y. Fukuda *et al.* (Super-Kamiokande), *Phys. Rev. Lett.* **81**, 1562 (1998), [hep-ex/9807003](#).
- [8] Y. Ashie *et al.* (Super-Kamiokande), *Phys. Rev.* **D71**, 112005 (2005), [hep-ex/0501064](#).
- [9] T. Araki *et al.* (KamLAND), *Phys. Rev. Lett.* **94**, 081801 (2005), [hep-ex/0406035](#).
- [10] S. Abe *et al.* (KamLAND), *Phys. Rev. Lett.* **100**, 221803 (2008), [0801.4589](#).
- [11] M. H. Ahn *et al.* (K2K), *Phys. Rev.* **D74**, 072003 (2006), [hep-ex/0606032](#).
- [12] P. Adamson *et al.* (MINOS), *Phys. Rev. Lett.* **101**, 131802 (2008), [0806.2237](#).
- [13] F. Ardellier *et al.* (2004), [hep-ex/0405032](#).
- [14] X. Guo *et al.* (Daya-Bay) (2007), [hep-ex/0701029](#).

beams nominal				
	$g_N/\bar{g}_N$	$g_T/\bar{g}_T$	$l$	$\mu$
$\{\bar{g}_N, \bar{g}_T\}$	2016.62	2012.55, 2015.85	3	0.017
$\{\bar{g}_N, g_T\}$	2016.60	2014.59	2	0.017
$\{g_N, \bar{g}_T\}$	2012.22, 2016.62	2012.41, 2015.73	4	0.017
$\{g_N, g_T\}$	2012.29, 2016.62	2014.59	3	0.017
beams nominal + reactors				
	$g_N/\bar{g}_N$	$g_T/\bar{g}_T$	$l$	$\mu$
$\{\bar{g}_N, \bar{g}_T\}$	2016.04	2010.69	2	0.067
$\{\bar{g}_N, g_T\}$	2016.09	2017.26	2	0.058
$\{g_N, \bar{g}_T\}$	2013.25, 2016.22	2010.77	3	0.066
$\{g_N, g_T\}$	2012.95, 2016.05	2015.89, 2017.25	4	0.041
beams upgraded				
	$g_N/\bar{g}_N$	$g_T/\bar{g}_T$	$l$	$\mu$
$\{\bar{g}_N, \bar{g}_T\}$	2017.07	2010.7, 2015.29	3	0.015
$\{\bar{g}_N, g_T\}$	2016.46, 2019.48	2014.63, 2018.17	4	0.019
$\{g_N, \bar{g}_T\}$	2011.61, 2016.56, 2019.54	2010.13, 2014.65, 2018.15	6	0.019
$\{g_N, g_T\}$	2010.52, 2016.44, 2020.13	2014.64, 2017.09, 2018.35	6	0.031
beams nominal + reactors				
	$g_N/\bar{g}_N$	$g_T/\bar{g}_T$	$l$	$\mu$
$\{\bar{g}_N, \bar{g}_T\}$	2017.09, 2019.45	2010.25	3	0.032
$\{\bar{g}_N, g_T\}$	2017.13, 2019.44	2016.81, 2019.83	4	0.004
$\{g_N, \bar{g}_T\}$	2011.66, 2017.23, 2018.52	2010.00, 2016.82, 2019.99	6	0.005
$\{g_N, g_T\}$	2010.88, 2017.1, 2019.46	2016.81, 2019.83	5	0.004

**Table 3:** Average over the 100 fittest individuals in each population. The options shown in Fig. 11 are underlined.

- [15] S.-B. Kim (RENO), AIP Conf. Proc. **981**, 205 (2008).
- [16] Y. Itow *et al.*, Nucl. Phys. Proc. Suppl. **111**, 146 (2001), [hep-ex/0106019](#).
- [17] I. Ambats *et al.* (NOvA) (2004), [hep-ex/0503053](#).
- [18] H. Minakata, H. Sugiyama, O. Yasuda, K. Inoue, and F. Suekane, Phys. Rev. **D68**, 033017 (2003), [hep-ph/0211111](#).
- [19] P. Huber, M. Lindner, and W. Winter, Nucl. Phys. **B654**, 3 (2003), [hep-ph/0211300](#).
- [20] P. Huber, M. Lindner, T. Schwetz, and W. Winter, Nucl. Phys. **B665**, 487 (2003), [hep-ph/0303232](#).
- [21] P. Huber, M. Lindner, M. Rolinec, T. Schwetz, and W. Winter, Phys. Rev. **D70**, 073014 (2004), [hep-ph/0403068](#).
- [22] K. B. McConnell and M. H. Shaevitz, Int. J. Mod. Phys. **A21**, 3825 (2006), [hep-ex/0409028](#).

- [23] M. Sanchez (MINOS), Talk given at Fermilab, 27 Feb. 2009.
- [24] G. Rosa (OPERA), J. Phys. Conf. Ser. **136**, 022015 (2008).
- [25] *European Commission FP7 Design Study: A High Intensity Neutrino Oscillation Facility in Europe*, <http://www.euronu.org>.
- [26] *International design study of the neutrino factory*, <http://www.ids-nf.org>.
- [27] P. Huber, M. Lindner, and W. Winter, Comput. Phys. Commun. **167**, 195 (2005), <http://www.mpi-hd.mpg.de/lin/globes/>, hep-ph/0407333.
- [28] P. Huber, J. Kopp, M. Lindner, M. Rolinec, and W. Winter, Comput. Phys. Commun. **177**, 432 (2007), hep-ph/0701187.
- [29] P. Huber, J. Kopp, M. Lindner, M. Rolinec, and W. Winter, JHEP **05**, 072 (2006), hep-ph/0601266.
- [30] G. Mention, T. Lasserre, and D. Motta (2007), 0704.0498.
- [31] M. Fechner, *Détermination des performances attendues sur la recherche de l'oscillation  $\nu_\mu \rightarrow \nu_e$  dans l'expérience T2K depuis l'étude des données recueillies dans l'expérience K2K*, Ph.D. thesis, Université Paris VI (2006).
- [32] I. Kato (T2K), J. Phys. Conf. Ser. **136**, 022018 (2008).
- [33] T. Yang and S. Wojcicki (NOvA) (2004), Off-Axis-Note-SIM-30.
- [34] *NOvA Technical Design Report, October 23, 2007*, [http://www-nova.fnal.gov/nova\\_cd2\\_review/tdr\\_oct\\_23/tdr.htm](http://www-nova.fnal.gov/nova_cd2_review/tdr_oct_23/tdr.htm).
- [35] T. Schwetz, M. Tortola, and J. W. F. Valle, New J. Phys. **10**, 113011 (2008), 0808.2016.
- [36] M. McFarlane, K. Heeger, P. Huber, C. Lewis, and W. Wang (2009), in preparation.
- [37] G. L. Fogli and E. Lisi, Phys. Rev. **D54**, 3667 (1996), hep-ph/9604415.
- [38] S. Antusch, P. Huber, J. Kersten, T. Schwetz, and W. Winter, Phys. Rev. **D70**, 097302 (2004), hep-ph/0404268.
- [39] S. Niehage and W. Winter, Phys. Rev. **D78**, 013007 (2008), 0804.1546.
- [40] S. Antusch, J. Kersten, M. Lindner, and M. Ratz, Nucl. Phys. **B674**, 401 (2003), hep-ph/0305273.
- [41] S. Peeters, *Seeking  $\theta_{13}$  with reactor neutrinos*, Talk given at NOW 2008 <http://www.ba.infn.it/~now/now2008/>.
- [42] R. McKeown, *The daya bay reactor neutrino experiment*, Talk given at CIPANP 2009, San Diego, USA <http://groups.physics.umn.edu/cipanp2009/>.

- [43] Y. Oh, *Current status of RENO*, Talk given at NOW 2008  
<http://www.ba.infn.it/~now/now2008/>.
- [44] H. Kakuno, *Neutrino oscillations at T2K*, Talk given at NOW 2008  
<http://www.ba.infn.it/~now/now2008/>.
- [45] M. Messier, *The NOvA Experiment at Fermilab*, Talk given at ICHEP 2008,  
<http://www.hep.upenn.edu/ichep08/talks/misc/schedule>.
- [46] T. Schwetz and W. Winter, Phys. Lett. **B633**, 557 (2006), [hep-ph/0511177](#).
- [47] J. Kopp, M. Lindner, T. Ota, and J. Sato, Phys. Rev. **D77**, 013007 (2008), 0708.0152.
- [48] T. Nakaya, private communication.
- [49] K. Hasegawa, *The j-parc neutrino beam*, Talk given at NNN 08, Paris France,  
<http://nnn08.in2p3.fr/> .
- [50] *Resource-loaded schedule*, director's Preliminary Cost and Schedule Review, March 16-17, 2009, <http://projectx.fnal.gov>.
- [51] H. Minakata and H. Sugiyama, Phys. Lett. **B580**, 216 (2004), [hep-ph/0309323](#).
- [52] W. Winter, Phys. Rev. **D70**, 033006 (2004), [hep-ph/0310307](#).